Ceramics International xxx (xxxx) xxx–xxx

Contents lists available at ScienceDirect

Ceramics International

journal homepage: www.elsevier.com/locate/ceramint

Phase, microstructural investigation and thermoelectric properties of Ga-doped zinc oxide-based ceramics sintered under an argon atmosphere

Mati Ullah[a], Wen Bin Su[a], Abdul Manan[b,*], Arbab Safeer Ahmad[c], Abid A. Shah[d], Zhonghua Yao[e]

[a] School of Physics, Shandong University, Jinan 250100, PR China
[b] Laboratory for Research in Advanced Materials, Department of Physics, University of Science and Technology Bannu, Bannu 28100, Khyber Pakhtunkhwa, Pakistan
[c] Department of Physics, Islamia College Peshawar, Peshawar 25120, Khyber Pakhtunkhwa, Pakistan
[d] Department of Civil Engineering, International Islamic University, Islamabad, Pakistan
[e] State Key Laboratory of Advanced Technology for Materials Synthesis and Processing, School of Materials Science and Engineering, Wuhan University of Technology, Wuhan 430070, China

ARTICLE INFO

Keywords:
Elements
Oxides
Electronic materials
Thermoelectrics

ABSTRACT

Compositions in the $(Zn_{0.98-y}Al_{0.02}Ga_y)O$ (y = 0.00, 0.01, 0.02, 0.03) series were fabricated via the conventional solid-state sintering route under an argon atmosphere, and their phase, microstructure and thermoelectric properties were investigated. Single-phase ceramics were formed for the compositions with $y \leq 0.01$. However, an unknown secondary phase was developed along with the parent phases when $y \geq 0.02$ due to an over solubility limit of Ga in Zn. For a particular value of Ga substitution for Zn, the $(Zn_{0.98}Al_{0.02})O$ ceramics had decreased electrical resistivity **(ρ)** and an increased power factor **(PF)**. In the present study, the highest power factor of 5.518×10^{-4} W K^{-2} m^{-1} and lowest electrical resistivity of ~0.82 mΩcm were obtained for the composition with y = 0.01, i.e., $(Zn_{0.97}Al_{0.02}Ga_{0.01})O$.

1. Introduction

In the recent years, thermoelectric technology has attracted great attention, as it can directly convert heat into electricity. The efficiency of thermoelectrics is improved by improving the materials, fabrication techniques, and devices. Some of the previously reported highly efficient thermoelectric compositions for power generation applications including half-Heuslers [1,2] and other classes as lead telluride [3] and germanium telluride [4]. However, ZnO has also been reported to be one of the best thermoelectric material, as it has a high Seebeck coefficient **(S).** Due to this tolerable value of S, the power factor of ZnO is higher than those of other thermoelectric materials. Thermoelectricity has a more than 150 year history, and it depends on three basic phenomena: the Thomson effect, Peltier effect and Seebeck effect [5,6]. Heat can be converted directly to electricity by the Seebeck effect. The main advantage of thermoelectric materials and devices is the absence of moving parts [7]. Thermoelectric oxide materials are well known to work at high temperatures, and they are stable at high temperatures, nontoxic [8] easily availability and inexpensive [9]. Zinc oxide is widely used in cement [10], gas sensors [11] and varistors [12,13]. Thermoelectric materials are useful for power generation due to their thermal stability. ZnO is one of the most suitable thermoelectric materials due to its unique properties, such as a high Seebeck coefficient and high carrier mobility values [14]. It is an n-type semiconductor with a band gap of 3.3 eV and has a wurtzite structure [15]. The lattice parameters of ZnO are a = 3.2488 Å and c = 5.2054 Å [16]. The high lattice thermal conductivity (K_L) is the main disadvantage of ZnO.

In 2011, S. Teehan studied the effect of In doping in ZnO on the ρ and power factor and obtained a **PF** of ~ 22.1×10^{-4} W K^{-2} m^{-1} and a ρ on the order of 2.1 mΩcm [17]. D. Berardan et al. studied $(Zn_{1-x}Al_x)O$ compositions prepared under air and under N_2 and obtained a lower ρ and a higher power factor for the samples sintered under N_2. A ρ of 2 mΩ cm and a **PF** of ~ 3.8×10^{-4} W K^{-2} m^{-1} were obtained for the nominal formula $(Zn_{0.98}Al_{0.02})O$ with x = 0.02 sintered under a N_2 atmosphere [13].

In previous studies, different techniques and sintering atmospheres have been implemented to reduce the ρ, but the reductions in electrical resistivity have remained limited. S. Yang et al. obtained a power factor of 5.3×10^{-4} W m^{-1} K^{-2} at 750 K for $Zn_{0.98}Al_{0.02}O$ ceramics [18]. D. B. Zhang et al. achieved a **PF** ~ 6.16×10^{-4} W m^{-1} K^{-2} for Ni, Al dual-doped ZnO [19].

In the present study $(Zn_{0.98}Al_{0.02}Ga_y)O$ ceramics were prepared by the traditional solid-state reaction method. The thermoelectric properties of the $(Zn_{1-x-y}Al_xGa_y)O$ ceramics were investigated between 100 and 700 °C.

* Corresponding author.
E-mail address: drmanan82@ustb.edu.pk (A. Manan).

https://doi.org/10.1016/j.ceramint.2018.06.259
Received 11 June 2018; Received in revised form 28 June 2018; Accepted 29 June 2018

2. Methods and material

Compositions with the nominal formula $(Zn_{1-x-y}Al_xGa_y)O$ with x = 0.02 and y = 0.00, 0.01, 0.02, 0.03 were processed via the solid-state sintering route by using high-purity raw materials, namely, ZnO (99%), Al_2O_3 (99%) and Ga_2O_3 (99.99%). The raw materials were weighed in stoichiometric ratios and ball milled for 15 h using ethanol as a lubricant and a zirconia ball as the grinding media. The slurries were dried in an oven to obtain powders. The powders were pressed into 12 mm diameter disks and sintered under an argon atmosphere at 1450 °C for 10 h. Phase analysis of the sintered samples was carried out by the X-ray diffraction (XRD) technique (D8 Bruker Toshiba Japan) with 2θ = 20–80° at a scan rate of 2° per minute and a step size of 0.02° by using Cu-Kα radiation.

The microstructure of all the sintered samples was examined using scanning electron microscopy (SEM, Hitachi S-480). The thermoelectric properties, such as resistivity, **SC** and **PF**, were measured from 100° to 700°C by an LSR-3 machine. All the measurements were performed from room temperature to 700 °C. The **SC** was obtained from the temperature difference between the upper and lower heaters of the LSR-3 machine. The obtained results were automatically transferred to the computer system by a 32-bit state-of-the-art software

3. Results and discussion

Fig. 1 shows the X-ray diffraction of all the sintered compositions in the $(Zn_{0.98}Al_{0.02}Ga_y)O$ (y = 0, 0.01, 0.02, 0.03) series. Powder X-ray diffraction of the $(Zn_{0.98}Al_{0.02}Ga_y)O$ ceramics with different amounts of Al and Ga are shown in Fig. 1. The sharpest peaks in the XRD patterns of all the compositions corresponding to the hexagonal wurtzite structure of the host ZnO and match with PDF#70-2551, corresponding to ZnO (zincite, sys). The shifting of the sharpest peaks towards smaller d values shows better crystallinity in the (101) direction, where (101) denotes the Miller indices (*hkl*). A single-phase ceramic formed for the compositions with y ≤ 0.01. The low-intensity peaks labeled **β** appeared for the compositions with y ≥ 0.02, indicating the formation of a secondary phase along with the parent phase. However, the nature of the secondary phase could not be identified. This unknown secondary phase might contain Ga. This result indicated that the solid solubility limit for Ga in Zn was ~ 1 mol%.

Fig. 2**(a)-(d)** shows the morphology and topography of $Zn_{0.98-y}Al_{0.02}Ga_yO$ observed by a scanning electron microscope (SEM-Hitachi S-4800). The results for all the compositions are in good agreement with the XRD findings. In the XRD patterns, the two low-intensity peaks

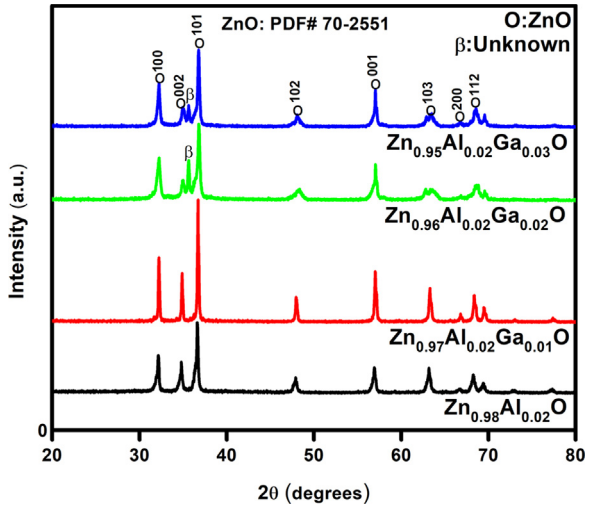

Fig. 1. Powder X-ray diffraction of $(Zn_{0.98-y}Al_{0.02}Ga_y)O$ ceramics (y = 0, 0.01, 0.02, 0.03).

represent the unknown phase labeled **β** for y ≥ 0.02. These unknown phase appearing at approximately 2θ = 35° are due to the Ga content. This observation revealed that the compositions with a higher amount of Ga dopant showed high porosity. The number of dark grains was increased with increasing Ga substitution. The granular size was probably increased due to the Ga impurity (Fig. 2 **c, d)**. The dark and increased granular texture was observed for compositions $(Zn_{0.98}Al_{0.02}Ga_y)$ when y = 0.00, 0.01, 0.02. 0.03. The Grass elemental compositions of Zn0.98-yAl0.02Ga0.98O (y = 0.00, 0.01, 0.02, 0.03) are given in Table 1.

Fig. 3 presents the variation in the electrical resistivity (ρ) of $(Zn_{0.98-y}Al_{0.02}Ga_y)O$ (y = 0.00, 0.01, 0.02, 0.03) ceramics. The ρ of all the compositions increased with increasing temperature. Therefore, the gradual increase in ρ with temperature has a positive temperature coefficient (PTC) [20]. The ρ of the composition with y = 0.03 has the highest value and increased from 3.974 mΩ cm at 101.4 °C to 4.277 m Ω cm at 692.7 °C. For the composition with y = 0.02, a similar increase in the ρ was also observed with increasing temperature. the ρ ranged from 3.564 mΩ cm at 101.1 °C to 3.993 mΩ cm at 692.3 °C. Similarly, for the composition with y = 0.01, the ρ increased from 0.872 mΩ cm at 101.6 °C to 1.194 mΩ cm at 693.4 °C. The ρ of the composition with y = 0 increased from 1.273 mΩ cm at 102.1 °C to 1.598 mΩ cm at 693.5 °C. A possible reason for the increase in ρ with increasing temperature was the maximum number of charge carriers, which increases the collision between the charge carriers. As a result, an increase in ρ was observed in this situation, as the semiconductor behaves like a metal. Doping elements such as Al and Ga have a greater atomic weight than Zn. In this case, the semiconductor behaves more similarly to a metal. This kind of semiconductor is called a degenerate semiconductor. In a degenerate semiconductor, the dopants create individually localized states. These localized states therefore donate electrons or holes to the conduction or valence band, respectively. In degenerate semiconductors, the number of charge carriers is still very low compared to that in real metals, so the degenerate semiconductor behavior in many ways is intermediate between a semiconductor and a metal.

The composition with y = 0.01 showed the lowest ρ among all the compositions. This indicated that for single-phase ceramic, the ρ was decreased with Ga substitution. However, the increase in ρ for the compositions with y ≥ 0.02 might be due to the formation of the unknown secondary phase that might have higher ρ than the parent phase.

With increasing temperature, oxygen vacancies were produced, and electrons were induced. The **S** of a semiconductor is higher than metals and alloys. At high temperatures, the induced electrons become thermal electrons, and hence, the ρ is increased due to electrons collision with each other and lattice. These electrons are now called conduction electrons (e^*). There is a strong relationship between these conduction electrons and oxygen vacancies (V_o^*). According to the Kroger-Vink notation given in Eq. (1) [21]

$$V_o = V_O^* + e^* \quad (1)$$

where V_o represents oxygen vacancies, e^* represents thermally activated electrons and V_O^* represents thermally induced oxygen vacancies. The increase in the number of conduction electrons (e^*) causing a semiconductor-to-metallic transition (SMT) [22,23]. To convert electron and holes to conduction electrons, approximately 1.1 eV of energy is required [24]. The conduction electrons play an important role in affecting the **S**.

Fig. 4 shows the variation in the **S** of $(Zn_{0.98-y}Al_{0.02}Ga_y)O$ (y = 0.00, 0.01, 0.02, 0.03) as a function of temperature, referred to as the thermoelectric effect [25]. All the compositions showed a negative value of **S**, indicating n-type conduction. The values of the **S** for all compositions steadily decreased with increasing temperature. The inverse relation between the **S** and the number of carriers is a general trend. The increase in temperature increases the number of carriers in the valance band. These charge carriers (thermally activated electrons) are now